

Differentiation of Hard Red Wheat by Near-Infrared Analysis of Bulk Samples

STEPHEN R. DELWICHE,¹ YUD-REN CHEN, and WILLIAM R. HRUSCHKA

ABSTRACT

Cereal Chem. 72(3):243-247

Near-infrared reflectance spectroscopy (1,100–2,498 nm) has been used to identify hard red winter and hard red spring wheat classes. As a follow-up to a previous study which involved ground wheat samples, the authors have used the same samples on a whole kernel in-bulk (80 g) basis. Four years of U.S. winter and spring wheats were used. A small number ($n = 150$ samples per class) from the first three years' samples were used for calibration; the remaining portion ($n = 1,325$), plus all of the fourth year's samples ($n = 778$), were used to verify the models. Four types of classification algorithms were examined: multiple linear regression (MLR), principal component analysis with Mahalanobis distance (PCA/MD), partial least squares (PLS) analysis, and artificial neural networks (ANN). All four models demonstrated classification accuracies (defined as the percentage of correctly classified samples) greater than 88%, and

most often, about 95% for samples grown during the same years as used in calibration. These accuracies were significantly better than those associated with discriminant models that were based solely on protein content, NIR-hardness, or a combination of protein and hardness. Spectrally sensed water-matrix interactions were probably beneficial to model accuracy; however, moisture content alone was not deemed necessary to a model's success. When predicting the fourth year, the MLR model needed a bias correction, whereas the other three models performed reasonably well. The ANN model's performance was highest, with accuracies in the range of 95–98%. At little expense to model accuracy, the number of input nodes to the ANN model could be reduced from 223 to 111, provided the full wavelength range was preserved.

Hard red winter (HRW) and hard red spring (HRS) are the two most prevalent classes of breadmaking wheats grown in the United States. The current market system for U.S. grown wheat for domestic and overseas markets is based on the usual segregation of wheat by class (Office of Technology Assessment 1989). In some years, a premium may be paid for HRS wheat due to a perceived higher breadmaking quality. Hence, buyers wish to maintain the traditional classification system. The United States Department of Agriculture, Federal Grain Inspection Service (FGIS) is responsible for the grading of all U.S. wheat sold for export and inspects samples in the domestic market on request. Classification is traditionally performed by trained personnel who examine the size, shape, color, and other physically distinct features of kernels in a sample of grain. Some subjectivity in class assignment is unavoidable. In the movement toward developing rapid, objective classification and grading methods, the FGIS has been seeking alternative methods to human visual inspection. To date, intact-kernel classification research has been based on digital image analysis of nontouching kernels (Zayas et al 1985, 1986; Neuman et al 1987; Sapirstein et al 1987; Symons and Fulcher 1988 a,b; Chen et al 1989; Thomson and Pomeranz 1991; Keefe 1992; Barker et al 1992 a–c) and touching kernels (Shatadal et al 1994).

Recently, we reported our results on developing a HRW/HRS classification system that is based on near-infrared (NIR) diffuse reflectance spectroscopy of ground wheat (Delwiche and Norris 1993). Non-mixed-class samples from four crop years were correctly classified as HRW or HRS at an accuracy of 95% by a technique based on the Mahalanobis distance of the sample scores from principal component analysis. Such accuracies were not attainable through simpler discriminant functions that employed either protein content, NIR-hardness, or a combination of both. Year-to-year changes in the average levels of these constituents for each class were the reason for the poorer performance of the simpler functions. We concluded that a full-spectrum technique such as principal component analysis on NIR spectra was necessary for robust classification; otherwise, yearly adjustments

to mean protein and hardness levels would be necessary. The current study differs from the previous one in that examination by NIR is performed on bulk wheat without first grinding the sample; however, the same samples that constituted the calibration, validation, and prediction sets have been used. If successful, classification by NIR spectroscopy would be advantageous over digital imaging in terms of equipment cost and computational processing time. The objectives of the current study were to develop accurate models for the differentiation of HRW and HRS wheats based on NIR reflectance spectra of bulk samples and to compare various classification algorithms. Although the scope of the study was limited because individual kernels were not examined and, hence, detection of mixtures of classes was not possible, the study represented the first comprehensive attempt to determine whether differences in intrinsic properties of the hard red wheat classes are measurable by NIR spectroscopy.

MATERIALS AND METHODS

Wheat Samples

Samples of HRW and HRS wheats from four crop years (1987–1991) were purchased from a private source (Doty Laboratories, Kansas City, MO). More than 600 samples per year were obtained as part of an annual crop survey of the hard red wheat growing region of the central United States. Classification was performed by field personnel at the time of collection and verified on two year's (1987, 1988) surveys by the FGIS Board of Appeals and Review. Each survey represented a very good compilation of the quality of U.S. grown hard red wheats for the given year. The ratio of the number of HRW to HRS samples was about 2 to 1, with the exception of one year in which only 81 HRS samples were available in sufficient quantity. Yearly means and standard deviations of protein content and NIR-hardness, as well as state origin of the samples from each class, are summarized in Delwiche and Norris (1993).

Equipment

A near-infrared spectrophotometer (model 6500, NIRSystems, Silver Spring, MD) equipped with a bulk transport cell attachment was used to collect reflectance spectra of bulk kernel samples. Wheat, with dockage and foreign material removed, was loaded into a rectangular prismatic cell (height 200 mm, width 38 mm, depth 14 mm). Approximately 80 g of seed was required to fill the cell to three-quarters height. Opposing height \times width faces were clad with infrared transmitting quartz windows (thickness

¹Instrumentation and Sensing Laboratory, Beltsville Agricultural Research Center, ARS, USDA, Beltsville, MD.

Mention of company or trade name is for purpose of description only and does not imply endorsement by the U.S. Department of Agriculture.

1.52 mm). Samples were scanned (1,100–2,498 nm wavelength range) in the reflectance mode and referenced to corresponding reflected energy readings from a ceramic block. Reflected energy was captured by two pairs of opposing lead sulfide detectors (each 10 mm × 10 mm) oriented 45° with respect to the incident radiation and placed ~20 mm from the near face of the sample cell. The incident radiation path and detector remained stationary while the sample cell moved downward at constant speed during scanning. The speed was adjusted so that 38 repetitive scans were performed in one downward movement of the cell. Scans were averaged and transformed to $\log(1/R)$, producing one spectrum of 700 points (at a uniform 2-nm wavelength spacing) per sample. Each sample was loaded and analyzed once.

Model Development

Using the same calibration-, validation-, and prediction-set structure as described in Delwiche and Norris (1993), 50 samples from each of the two classes and from each of the first three crop years (1987–89) formed the calibration set (300 samples total). The remaining samples from 1987–89 (total = 1,325) formed the validation set. The fourth year's samples, of which none were used in calibration, formed the prediction set (total = 778).

As determined in preliminary analyses of bulk wheat spectra, a second-difference transformation on the spectra performed prior to spectral decomposition enhanced the discriminant functions, despite the appearance of a greater divergence in HRW and HRS in the raw spectra (Fig. 1). Although an offset in absorbance for the HRW and HRS mean spectra occurred throughout the entire wavelength region (upper graph), sample-to-sample spectral variation was large enough to produce spectral overlap of the two classes when individual samples were examined. Second-difference spectra were more effective at accentuating the class differences in individual samples. Consequently, all discriminant modeling was preceded by the application of a three-point central second difference to the raw $\log(1/R)$ spectral data:

$$g(\lambda_i) = k[f(\lambda_{i+j}) - 2f(\lambda_i) + f(\lambda_{i-j})]$$

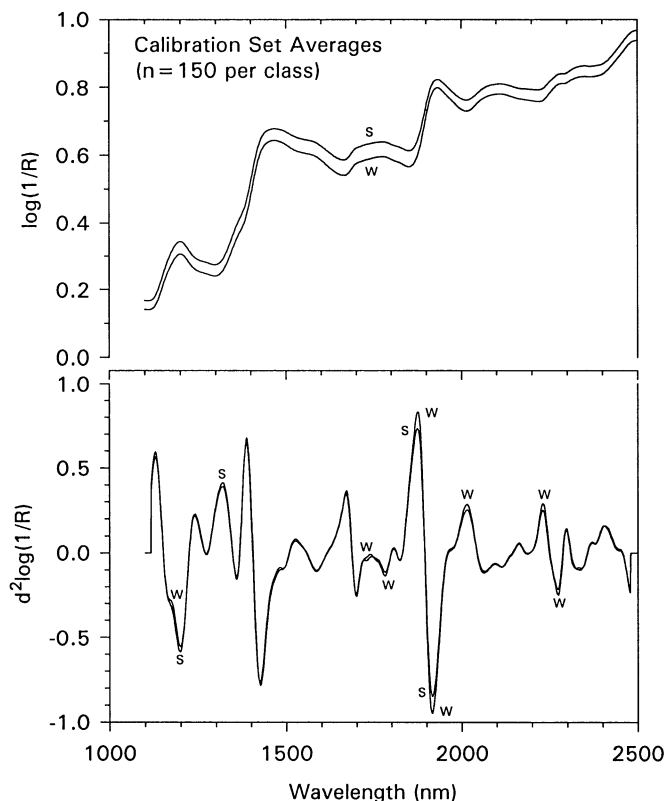


Fig. 1. Average spectra (top graph) of the calibration set. Set consisted of 150 samples of hard red winter (W) and 150 samples of hard red spring (S) wheats from 1987–1989 crop years. Three-point central second differences (gap = 20 nm) of spectra in bottom graph.

where $g(\lambda)$ is the second-difference spectrum, $f(\lambda)$ is the spectrum before transformation, k is a scaling constant, i is the wavelength index, and $j = 10$ is the gap (i.e., the half-width expressed in points) of the finite difference window. Generally, a second-difference transformation greatly eliminates spectrum-to-spectrum baseline differences, which is advantageous in the case of ground samples for reducing the effect of differences in light scatter caused by different particle size distributions (Hruschka 1987). Similar benefits were found on bulk samples.

For purposes of reducing required computer memory and enhancing speed, every third point within the second-difference spectrum was stored, while the remaining points were discarded. Thus, each sample was represented by 223 second-difference values over the range 1,136–2,468 nm at a constant spacing of 6 nm. Preliminary analyses indicated that this form of data compression could be performed without detrimental effects, owing to the collinearity of neighboring wavelength points.

Four classification models were examined: multiple linear regression (MLR), principal component analysis with Mahalanobis distance classifier (PCA/MD), partial least squares (PLS), and artificial neural networks (ANN). Classification accuracies of these spectral models were compared with previously reported accuracies (Delwiche and Norris 1993) associated with simple linear discriminant functions that were based on protein content, NIR-hardness, or a combination of these constituents.

Conditions for MLR Modeling

HRW and HRS samples were assigned the arbitrary values 0.0 and 1.0, respectively. Stepwise multiple linear regression was applied to the calibration set to determine the best one-, two-, three-, and four-term models, having the general form:

$$Class = k_0 + k_1 g_1 + \dots + k_i g_i$$

where second differences are designated as g_1 and g_i , and constants are k_0 , k_1 , and k_i . The equations were subsequently applied to the validation and prediction sets, such that a sample was assigned to HRW when $Class \leq 0.5$ and to HRS when $Class > 0.5$. Model accuracies were determined as the percentages of HRW and HRS samples correctly determined.

Conditions for PCA/MD Modeling

Before application of the discriminant function, the calibration-set spectra were decomposed into their principal components, as described in Lindberg et al (1983). Each spectrum's scores (i.e., the coefficients for each sample, such that when multiplied by their corresponding eigenvector and summed, the spectrum could be reproduced to within a small error) were used as input to development of the discriminant function. Separate decompositions were performed on the two wheat classes. When each sample's scores were plotted in multidimensional space, the nearness of each sample to the group mean was determined in standard deviation (i.e., Mahalanobis distance) units. These distances were then normalized against all samples within the calibration set of each class, thereby permitting comparisons between classes with different magnitudes of standard deviation.

Upon forming a discriminant function for each class, all samples from the validation and prediction sets were tested using the two discriminant functions. Assignment of a sample to the winter or spring class was based upon the normalized Mahalanobis distance to the two groups' means. For each sample, the class with the smaller distance was then assigned to the sample. The same procedure was used in Delwiche and Norris (1993). Computations were performed using the Discrim routine of an MS-DOS spectral analysis program (Lab Calc, Galactic Industries, Salem, NH).

Conditions for PLS Modeling

Spectral decomposition was performed in the same manner as the PCA/MD method, with the difference that both winter and spring calibration samples were grouped together. Furthermore, wavelength regions that demonstrated the most difference

between winter and spring samples were preferentially weighted during formation of the factors in the manner that defines the difference between the PLS and PCA algorithms (Lindberg et al 1983). As in the MLR model, winter and spring samples were assigned the values 0.0 and 1.0, respectively. Likewise, model accuracy was determined as the percentage of winter samples within a set that were predicted to have a value less than or equal to 0.5 (the midpoint) and of spring samples with a value greater than 0.5. Models of up to 10 factors were examined. A commercial MS-Windows program (GRAMS/386, Galactic) was used to develop the models.

An additional PLS model, which excluded the two wavelength regions of water absorption (1,348–1,500 and 1,830–1,960 nm) in the second-difference data, was examined for the purpose of assessing the importance of moisture content in the accuracies of the full-spectrum models. Ideally, a robust model should not be reliant on differences between mean moisture contents of the two classes caused by different crop management practices at time of harvest or differences in postharvest handling. Therefore, a similarity in accuracies between this additional model and the fuller wavelength PLS model would support an argument that moisture content alone is not primarily responsible for successful differentiation of HRW and HRS wheats.

Conditions for ANN Modeling

Calibration samples from both classes were the input to a feed-forward back-propagation model (Hecht-Nielsen 1989). The input layer consisted of 223 nodes, with each wavelength of the compressed second difference spectrum occupying one node. Two nodes representing the HRW and HRS wheat classes formed the output layer. Modeling was initially performed with and without an intermediate (hidden) layer of nodes. Because intermediate-layer models did not demonstrate performance superior to those without one, the intermediate layer was not used in subsequent analyses. A sigmoidal activation function was applied to each node of the output and intermediate layers. The learning rate and momentum were initialized at 0.9 and 0.6, respectively. Up to 50,000 iterations were allowed during training. Software running in the MS-DOS environment was used (Neuralworks Professional II/Plus, Neuralware, Inc., Pittsburgh, PA). A thorough discussion on the application of this algorithm to wheat classification is given in Song et al (*in press*).

RESULTS AND DISCUSSION

General

A summary of the model performance for the four types of

spectral models and for the constituent-based models is shown in Table I. Model accuracy (i.e., percent of correctly classified samples) is listed for each of the two classes. The average of the two accuracies is also listed and represents a figure of merit independent of the proportion of HRW to HRS samples.

All four spectral models demonstrated that calibration samples could be correctly assigned to their actual classes at least 90% of the time, and in most cases in excess of 95% of the time. Assuming a 2–3% classification error for what is designated in Table I as the "Actual Class" (Delwiche and Norris 1993), validation and prediction set accuracies of 97% are probably at the upper limit.

Whereas all of the spectral models demonstrated calibration- and validation-set accuracies in excess of 90% (with exception of the PCA/MD model on the HRS validation set), none of the protein content, NIR-hardness, or combination of protein and NIR-hardness models had such accuracies on corresponding sets. Instead, model accuracies of the constituent models were typically about 85%. Constituent model accuracies were higher on the prediction set, which was formed from the 1990 crop year, primarily because the mean values for protein content of those samples (HRW = 13.4%, HRS = 16.0%) were relatively close to the corresponding mean values for the preceding three years combined, which formed the calibration and validation sets, despite the large range in yearly mean protein contents (HRW = 12.1% [1987] to 14.5% [1989], HRS = 14.7% [1987] to 17.0% [1988] from Table I in Delwiche and Norris 1993). The prediction set accuracies of the constituent models were still generally lower than the prediction set accuracies of the PCA/MD, PLS, or ANN models. Thus, these full spectral models appear to be necessary to ensure invariance in accuracy from year to year.

The accuracy of classifying the HRS prediction samples dropped to less than 90% for the PCA/MD model. Surprisingly, the MLR model, which was the simplest spectral model, demonstrated accuracies on the calibration and validation sets that were within 0.6–4.0% of the accuracies for the two most mathematically complex models, the PLS and ANN models. Of the various (one to four wavelength) MLR trials examined, a three-term second-difference ($\lambda = 1,262, 1,798, \text{ and } 2,336 \text{ nm}$) model yielded the highest validation set accuracy and, consequently, it is the MLR model shown in Table I. The MLR model accuracy was affected by the introduction of the new crop year, as demonstrated by an imbalance in prediction set classification accuracy between the HRW samples (100%) and the HRS samples (24.1%). Upon examining the values for *Class* (equation 2), it was found that a positive bias occurred in the prediction set samples. Changing

TABLE I
Summary of Model Performances for Hard Red Winter (HRW) and Hard Red Spring (HRS)

Set	Actual Class	n	On Constituents, Using Linear Discriminant Functions ^a			On Spectral Data				
			Protein Content	NIR Hardness	Protein & Hardness	MLR ^b (3-term)	PCA/MD ^c (8-factor)	PLS ^d (7-factor)	PLS ^e (7-factor, less H ₂ O absorption regions)	ANN ^f (9,900 iterations)
Calibration	HRW	150	84.0	85.3	87.3	96.0	95.3	98.0	97.3	98.0
	HRS	150	84.0	87.3	88.7	94.7	90.7	98.0	97.3	98.7
	Average		84.0	86.3	88.0	95.3	93.0	98.0	97.3	98.3
Validation	HRW	892	79.9	86.2	88.5	96.7	92.4	97.3	97.4	97.9
	HRS	433	76.5	86.4	82.9	93.3	88.4	95.2	94.4	94.9
	Average		78.2	86.3	85.7	95.0	90.5	96.2	95.9	96.4
Prediction	HRW	471 ^g	91.9	68.5	86.2	100.0 (95.4) ^h	92.6	91.3	84.9	96.6
	HRS	207 ^g	90.3	94.9	97.7	24.1 (95.3)	95.6	98.6	98.6	98.0
	Average		91.1	81.7	92.0	62.1 (95.4)	94.1	94.9	91.8	97.3

^a Values derived from Table II of Delwiche and Norris (1993).

^b Multiple linear regression. The three terms were second differences of $\log(1/R)$ at 1,262, 1,798, and 2,336 nm, with coefficients equaling 1,139.69, 954.98, and -389.08, respectively, and a constant of -3.83 (modeling HRW = 0.0; HRS = 1.0).

^c Principal component analysis with Mahalanobis distance classifier.

^d Partial least squares.

^e Same model as above, excluding 1,348–1,500 nm and 1,830–1,960 nm wavelength regions.

^f Artificial neural network, feed-forward back-propagation paradigm.

^g Prediction sets for the MLR and ANN models had an additional 50 samples, yielding $n = 521$ and 257 for the HRW and HRS sets, respectively.

^h Values in parentheses are accuracies of the MLR model after bias adjustment (i.e., changing constant from -3.83 to -3.18).

the value of k_0 from -3.83 to -3.18 for the prediction set improved the classification accuracy on this set to 95.4% for HRW and 95.3% for HRS samples. Only the ANN model demonstrated a higher combined accuracy for the two classes. The fact that a bias adjustment to the MLR model was necessary on the 1990 samples is supportive of the earlier statement claiming that full spectral models ensure yearly invariance.

The choice of seven factors as the optimal number for the PLS model was made by examining the accuracies associated with the validation and prediction sets as the number of factors varied (Fig. 2). Whereas validation set accuracy continued to improve up to nine factors, the prediction set accuracy declined after seven factors. Hence, a HRW/HRS PLS classification model involving more than seven factors would be overfitted to the climatic conditions of the crop years for which it was developed. By analogous reasoning, a plot of validation and prediction set accuracies versus the number of iterations for the ANN model (Fig. 3) demonstrated that, at 9,900 iterations, the model was stable. Further iteration resulted in a slight decline of prediction set accuracy.

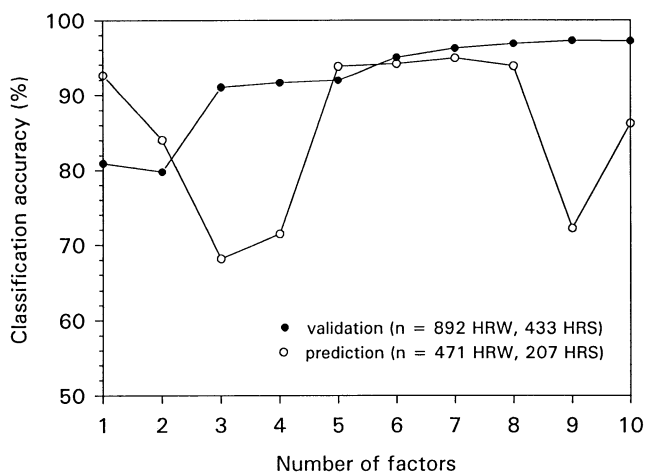


Fig. 2. Classification accuracy of a partial least squares (PLS) model as a function of the number of PLS factors used. Accuracy calculated as the average of the percentage of hard red winter (HRW) and hard red spring (HRS) samples correctly classified. Model conditions: 223 second difference of $\log(1/R)$ values, 1,136–2,464 nm, at increments of 6 nm.

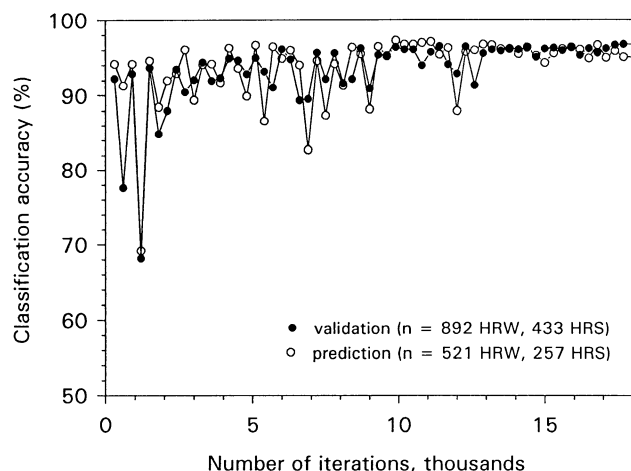


Fig. 3. Classification accuracy of an artificial neural network (ANN) as a function of the number of iterations utilized during training. Accuracy calculated as the average of the percentage of hard red winter (HRW) and hard red spring (HRS) samples correctly classified. Input nodes: 223 second difference of $\log(1/R)$ values, 1,136–2,464 nm, at increments of 6 nm.

Moisture Effects

The accuracies of the seven-factor PLS model that excluded the water absorption regions are displayed alongside the accuracies of the full spectrum PLS model (Table I). Although numerous wavelength regions exist throughout the NIR region that are identified with water (Williams and Norris 1987), the two excluded regions (1,348–1,500 and 1,830–1,960 nm) represent the most prominent absorption regions for pure water. Therefore, the intention of developing the model that excluded the water absorption regions was to minimize the direct effect of sample moisture while keeping the secondary effects of water-matrix interactions. With the exception of the HRW prediction set samples, accuracies of the model that excluded the water absorption regions were nearly identical to those of the full model. The reason for the lower accuracy rate of this set (84.9 vs. 91.3 % for models without H₂O and full models, respectively) is unclear. However, the fact that the accuracies of the two models were equivalent supports the argument that successful classification did not arise from class-specific differences in moisture content. These findings are in agreement with our earlier work on ground wheat (Delwiche and Norris 1993), in which we concluded that water-matrix interactions were more important for determining class than was water alone.

ANN Models

Additional ANN trials (Table II) were performed to examine the effects of using only the lower wavelength region (1,136–1,802 nm, $n = 112$ input nodes), using the upper wavelength region (1,808–2,468 nm, $n = 111$ input nodes), using the full region but with half the number of input nodes ($n = 112$), and manually eliminating certain wavelengths ($n = 78$) from the full region, half input node, model. In all trials, the purpose was to determine the extent to which classification accuracy declined when less than the full portion of the wavelength region was utilized. The number of iterations, as listed in Table II (5,400 for the upper and lower wavelength region models and 6,000 for the other models), represent the values at which accuracies had stabilized, such that additional iteration did not, on average across validation and prediction sets, improve the performance of the models.

The upper wavelength region model was more accurate than was the lower wavelength region model, as seen in the higher classification accuracies for all three sets (calibration, validation, and prediction), with exception of the HRS calibration set for which the accuracy of the two regions was equal. However, the upper region model was not as accurate as the ANN model employing the full wavelength region (Table I); the difference

TABLE II
Summary of Various Trials of ANN Modeling for Hard Red Winter (HRW) and Hard Red Spring (HRS)

Set	Actual Class	n	Classification Accuracy, Percent Correct ANN Model (number of iterations)			
			Lower Half ^a (5,400)	Upper Half ^b (5,400)	2× Spacing ^c (6,000)	Pruned ^d (6,000)
Calibration	HRW	150	90.7	93.3	92.7	92.0
	HRS	150	95.3	95.3	98.0	98.0
	Average		93.0	94.3	95.3	95.0
Validation	HRW	892	89.8	96.5	94.8	94.4
	HRS	433	91.7	92.6	95.6	94.7
	Average		90.7	94.6	95.2	94.5
Prediction	HRW	521	60.8	67.8	94.2	97.5
	HRS	257	99.2	99.6	98.4	88.7
	Average		80.0	83.7	96.3	93.1

^aWavelength range of input nodes: 1,136–1,802 nm; increment = 6 nm ($n = 112$).

^bWavelength range of input nodes: 1,808–2,468 nm; increment = 6 nm ($n = 111$).

^cWavelength range of input nodes: 1,136–2,468 nm; increment = 12 nm ($n = 111$).

^dWavelength range of input nodes: 1,136–2,468 nm; increment = 12 nm, with 36 nodes manually eliminated ($n = 75$).

in accuracies between the two models for the calibration and validation sets ranged from 1.4% (HRW of validation) to 4.7% (HRW of calibration). Furthermore, the large imbalance in accuracy rate between the HRW and HRS classes of the prediction set of the upper wavelength region model (67.8 vs. 99.6%, respectively) was suggestive of a bias being introduced in a new crop year's data. A better way of reducing the number of input nodes was by maintaining the full wavelength region, but doubling the wavelength distance between neighboring nodes, thereby reducing the number of nodes from 223 to 111. While accuracies were lower (with exception of the HRS validation and prediction sets) than if all nodes had been used, bias problems with the new crop year were not evident. Further reduction in the number of input nodes by manual removal (i.e., pruning of 36 low-weighted nodes, yielding 75 input nodes), resulted in a model with calibration- and validation-set accuracies comparable to those of the nonpruned model. However, the low prediction set accuracy for the pruned model (average = 93.1%) compared to that of the nonpruned version (average = 96.3%) suggests a decline in model robustness.

CONCLUSIONS

Classification of HRW and HRS wheats was accomplished on bulk samples by near-infrared reflectance. Depending on the discrimination algorithm, classification accuracies typically varied between 91 and 98%, as determined on sets of wheat samples excluded from calibration, as well as sets representing new crop years. Such accuracies were approximately 10 percentage points higher than our previously reported accuracies for discriminant functions that were based on protein content, NIR hardness, or a combination of both. The classification algorithms were as simple as a three-term multiple linear regression of second-difference values; however, such a model had to be bias-corrected when applied to a new crop year. The best models were based on artificial neural network (ANN) classifiers using a feed-forward back-propagation paradigm. Of the ANN models, the highest accuracies occurred when the full NIR spectrum was used (1,100-2,498 nm). In addition, accuracy was diminished only slightly upon widening the wavelength spacing between neighboring nodes of the second-difference spectra from 6 to 12 nm, thereby reducing the number of input nodes to 111. Additional reductions in the number of input nodes were possible with a slight decline in model accuracy by manual removal of nodes whose weights indicated minimal contribution to the outcome decision during calibration development. The success of spectrally based differentiation of HRW and HRS wheats did not appear to be caused by possible differences in mean moisture levels of the two classes.

This study represents the first attempt to determine whether official classification of U.S. wheats by NIR analysis on whole kernels might be possible. The promising results on bulk samples of whole grain reported herein have led to recently completed (Song et al, *in press*) and ongoing NIR classification studies on single kernels of wheat.

ACKNOWLEDGMENTS

We thank Joyce Shaffer and Minh Nguyen, USDA-ARS, for data collection and data analysis by neural networks, respectively.

- BARKER, D. A., VUORI, T. A., HEGEDUS, M. R., and MYERS, D. G. 1992a. The use of ray parameters for the discrimination of Australian wheat varieties. *Plant Var. Seeds* 5:35-45.
- BARKER, D. A., VUORI, T. A., and MYERS, D. G. 1992b. The use of slice and aspect ratio parameters for the discrimination of Australian wheat varieties. *Plant Var. Seeds* 5:47-52.
- BARKER, D. A., VUORI, T. A., and MYERS, D. G. 1992c. The use of Fourier descriptors for the discrimination of Australian wheat varieties. *Plant Var. Seeds* 5:93-102.
- CHEN, C., CHIANG, Y. P., and POMERANZ, Y. 1989. Image analysis and characterization of cereal grains with a laser range finder and camera contour extractor. *Cereal Chem.* 66:466-470.
- DELWICHE, S. R., and NORRIS, K. H. 1993. Classification of hard red wheat by near-infrared diffuse reflectance spectroscopy. *Cereal Chem.* 70:29-35.
- HECHT-NIELSEN, R. 1989. *Neurocomputing*. Addison-Wesley: New York.
- HRUSCHKA, W. R. 1987. Data analysis: Wavelength selection methods. Page 35 in: *Near-Infrared Technology in the Agricultural and Food Industries*. P. C. Williams and K. H. Norris, eds. Am. Assoc. Cereal Chem.: St. Paul, MN.
- KEEFE, P. D. 1992. A dedicated wheat grain image analyser. *Plant Var. Seeds* 5:27-33.
- LINDBERG, W., PERSSON, J. A., and WOLD, S. 1983. Partial least-squares method for spectrofluorimetric analysis of mixtures of humic acid and ligninsulfonate. *Anal. Chem.* 55:643-648.
- NEUMAN, M., SAPIRSTEIN, H. D., SHWEDYK, E., and BUSCHUK, W. 1987. Discrimination of wheat class and variety by digital image analysis of whole grain samples. *J. Cereal Sci.* 6:125-132.
- OFFICE OF TECHNOLOGY ASSESSMENT. 1989. Enhancing the quality of U.S. grain for international trade. Pages 189-215 in: *OTA-F-399*. GPO: Washington, DC.
- SAPIRSTEIN, H. D., NEUMAN, M., WRIGHT, E. H., SHWEDYK, E., and BUSHUK, W. 1987. An instrumental system for cereal grain classification using digital image analysis. *J. Cereal Sci.* 6:3-14.
- SHATADAL, P., JAYAS, D. S., and BULLEY, N. R. 1994. Segmentation of connected cereal grain images. *Am. Soc. Agric. Eng. Paper* 94-3022. The Society: St. Joseph, MI.
- SONG, H. P., DELWICHE, S. R., and CHEN, Y. R. In press. Neural network classification of wheat using single kernel near-infrared transmittance spectra. *J. Opt. Eng.*
- SYMONS, S. J., and FULCHER, R. G. 1988a. Determination of wheat kernel morphological variation by digital image analysis: I. Variation in Eastern Canadian milling quality wheats. *J. Cereal Sci.* 8:211-218.
- SYMONS, S. J. and FULCHER, R. G. 1988b. Determination of wheat kernel morphological variation by digital image analysis: II. Variation in cultivars of soft white winter wheats. *J. Cereal Sci.* 8:219-229.
- THOMSON, W. H., and POMERANZ, Y. 1991. Classification of wheat kernels using three-dimensional image analysis. *Cereal Chem.* 68:357-361.
- WILLIAMS, P. C., and NORRIS, K. H. 1987. Qualitative applications of near-infrared reflectance spectroscopy. Page 246 in: *Near-Infrared Technology in the Agricultural and Food Industries*. P. C. Williams and K. H. Norris, eds. Am. Assoc. Cereal Chem.: St. Paul, MN.
- ZAYAS, I., POMERANZ, Y., and LAI, F. S. 1985. Discrimination between Arthur and Arkan wheats by image analysis. *Cereal Chem.* 62:478-480.
- ZAYAS, I., LAI, F. S., and POMERANZ, Y. 1986. Discrimination between wheat classes and varieties by image analysis. *Cereal Chem.* 63:52-56.

[Received August 26, 1994. Accepted January 4, 1995.]